Full Paper

Journal of the Brazilian Chemical Society

https://dx.doi.org/10.21577/0103-5053.20260041

J. Braz. Chem. Soc. **2026**, *37-Spe1*, e-20260041, 1-9
©2026 Sociedade Brasileira de Química

Bioanalytical Studies in the Brain of Wistar Rats (*Rattus norvegicus*) Exposed to 2,3-Butanedione

Lucas X. Araújo,[a,b] *Letícia Gaiola,*[a,b] *Vinicius G. Ferreira,*[a,b] *Sinara T. B. Morais,*[a,b] *Nilson A. Assunção*[*,c] *and Emanuel Carrilho*[a,b]

[a]*Instituto de Química de São Carlos, Universidade de São Paulo, 13566-590 São Carlos-SP, Brazil*

[b]*Instituto Nacional de Ciência e Tecnologia de Bioanalítica Lauro Kubota (INCTBio-LK), 13083-590 Campinas-SP, Brazil*

[c]*Instituto de Ciências Ambientais, Químicas e Farmacêuticas, Universidade Federal de São Paulo, 09913-030 São Paulo-SP, Brazil*

2,3-Butanedione is widely used as a flavoring, preservative, and fragrance additive, and increasing evidence suggests that chronic exposure may induce molecular alterations in biological systems. This exploratory study investigated the impact of prolonged 2,3-butanedione exposure on the brain proteomic profile of Wistar rats. Thirty-three animals were assigned to three groups: a vehicle-treated control and two exposed groups receiving 46.6 or 99.1 μg kg^{-1} day^{-1} via intragastric administration for 90 days. Following euthanasia under deep anesthesia, brain tissues were analyzed by nano-liquid chromatography-mass spectrometry (nano-LC-MS), and the resulting data were evaluated using chemometric approaches. Data processing in Skyline identified 9,296 proteins, of which 2,500 were retained for multivariate analysis. Clear discrimination among experimental groups was observed, even in the absence of sex stratification, indicating that exposure influenced the global brain proteomic profile. Ontological and pathway analyses revealed 78 affected protein classes, with several dysregulated proteins annotated to biological pathways previously implicated in neurological processes. Importantly, these proteomic alterations represent pathway-level associations and do not constitute evidence of neurological disease or pathology. Overall, the findings demonstrate that chronic exposure to 2,3-butanedione modulates brain proteomic patterns and associated molecular pathways, supporting its use as a hypothesis-generating framework for future mechanistic and functional studies.

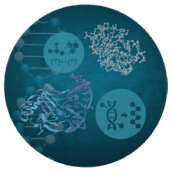

Keywords: proteins, 2,3-butanedione, mass spectrometry, mouse-brain, nano liquid chromatography

Introduction

2,3-Butanedione, widely used in the food industry, acts as a preservative and flavoring agent,[1,2] imparting an artificial buttery taste to foods.[3] This compound can be found in cocoa,[4] coffee,[5] alcoholic beverages[6,7] and dairy products.[8] In the pharmaceutical and cosmetics industry, it is used as a preservative in medicines,[9] a component of fragrances,[9] a photosensitizer in dental resin polymerization,[10,11] and an antimicrobial agent[12] effective against both Gram-positive and Gram-negative bacteria.[13]

In addition to being present in industrial processes, 2,3-butanedione can be found in conventional and electronic cigarettes (e-cigarettes).[14] E-cigarettes are very popular among young people; however, the effects that 2,3-butanedione can have on the brain are still poorly understood.

Previous *in vitro* results from the research group showed that 2,3-butanedione generates acetyl radicals, promoting non-enzymatic acetylation of proteins and deoxyribonucleic acid (DNA). Massari *et al.*[15] demonstrated that, in an oxygen-rich environment, peroxynitrite reacts with 2,3-butanedione to yield acetate. What occurs in an environment containing L-histidine or 2'-deoxyguanosine provides acetylation of these compounds. In 2010, Massari *et al.*[16] demonstrated the possible route of

*e-mail: nilson.assuncao@unifesp.br
Editor handled this article: Alessandra Sussulini (Guest) and Brenno A. D. Neto (Editor-in-Chief)
This publication is part of the special issue "Omics Sciences"

This is an open-access article distributed under the terms of the Creative Commons Attribution License.

acetylation of L-lysine using the methylglyoxal oxidation mechanism, when in an environment with peroxynitrite and molecular oxygen, it can release acetate and formate via an acetyl radical intermediate.

In terms of brain damage, in 2012, More *et al.*[17] used an *in vitro* model of the blood-brain barrier to demonstrate that 2,3-butanedione can accelerate the aggregation of β-amyloid (the main constituent of amyloid plaques observed in brains of Alzheimer's patients).[18] The authors also point out that 2,3-butanedione inhibits glyoxalase I, the primary enzyme that initiates the detoxification of reactive amyloid-promoting species.[17]

Literature data support the hypothesis that 2,3-butanedione can alter the structure and function of specific cellular macromolecules and may cause damage to individuals frequently exposed to it.[19-22] Despite this, little is known about how it acts in the brains of organisms.

In view of the *in vitro* evidence reported in the literature and the widespread presence of this substance in society, the present study was designed as an exploratory, hypothesis-generating proteomic investigation to the estimated daily intake in European Union (46,610 μg kg^{-1} day^{-1}; group 1) and North America (99,132 μg kg^{-1} day^{-1}; group 2), in comparison with a vehicle-treated control group, without the assessment of behavioral, histological, or functional neurological endpoints.

Experimental

Reagents and standards

All reagents had a purity greater than 95%, including urea, thiourea, 3-[(3-cholamidopropyl) dimethylammonio]-1-propanesulfonate (CHAPS), protease inhibitor cocktail, tris-base, trifluoroacetic acid (TFA), dithiothreitol (DTT), calcium chloride, iodoacetamide (IAA), trypsin, and Lys-C (Sigma-Aldrich, USA; Roche Diagnostics, Germany). High-performance liquid chromatography mass spectrometry (HPLC)-grade acetone and acetonitrile (LiChrosolv, Germany), formic acid (MS grade), and ultrapure water were also used.

For the Bradford assay, albumin (BSA) (Sigma-Aldrich, USA) was used, and the Bradford reagent (BioRad Protein Assay, USA).[23] To clean the glassware, Extran MA-01® alkaline detergent (Merck, Germany) and ethyl alcohol (Merck, Germany) were used.[24]

Mouse model development

All procedures used in the present study were performed in accordance with the guidelines established by the Brazilian College of Animal Experimentation (COBEA) and were approved by the Ethical Committee of the School of Medicine of the Federal University of São Paulo (UNIFESP); protocol No. 1949/11.

Eight- to twelve-week-old Wistar rats were divided into three groups of 11 animals each (five males and six females). The animals were housed under controlled conditions (50-70% humidity, 19-26 °C, 12 h light/dark cycle) and fed *ad libitum.* The rats received two different doses of 2,3-butanedione for eight weeks.

The treatment groups were as follows: a control group that received only phosphate-buffered saline solution (PBS); group 1 that received 46.6 μg (2,3-butanodione dissolved in PBS solution) kg^{-1} (animal weight) day^{-1}; and group 2 that received 99.1 μg kg^{-1} day^{-1} through gavage. After eight weeks of treatment, the animals were anesthetized with isoflurane and sacrificed. The brains were collected and stored at –80 °C until analysis.

Sample preparation

Samples were ground into a fine powder using a mortar and pestle and liquid nitrogen. This homogenization process was performed to inhibit protease activity and prevent protein degradation. After milling, the samples were lyophilized to remove residual water and stabilize them, allowing handling at room temperature and facilitating the weighing and extraction of analytes. Controls were carried out to ensure quality (QC) using aliquots of the same volume from each sample, containing all the study subjects; analytical blanks were also prepared to assess possible contamination of glassware or equipment.

Proteomic analysis

An aliquot of 15.0 mg were solubilized in the extraction buffer (7.0 mol L^{-1} of urea, 2.0 mol L^{-1} of thiourea, tris base 0.015 mol L^{-1}, pH 8.5, 4% (m/v) CHAPS, protease inhibitor cocktail, 0.1 mol L^{-1} DTT) and stirred for one hour using an Eppendorf shaker. Then, the homogenized sample was subjected to ultrasound pulses (3 s pulse and 15 s rest) for 5 min. After sonication, the sample was centrifuged (14,500 × g, 10 min, 4 °C), and the supernatant was recovered.

Proteins were precipitated with a solution of 2.0 mg mL^{-1} of DTT in acetone ice in the proportion of 1 part of sample to 3 parts of acetone/DTT. The solution was incubated overnight at 4 °C and centrifuged the next day (14.000 × g, 10 min, 4 °C).

The precipitate was washed thoroughly with the same solution containing 2.0 mg mL^{-1} DTT in ice-cold acetone.

After washing, the acetone was removed, the precipitate was dried under nitrogen, and the precipitate was solubilized in urea buffer (7.0 mol L^{-1} urea, 2.0 mol L^{-1} thiourea, tris base 0.015 mol L^{-1}, pH 8.5, 4% (m/v) CHAPS). After complete solubilization, the sample was centrifuged (12,000 rpm, 10 min, 4 °C) and the supernatant recovered.

Total protein concentration was determined by the Bradford method, with correction for interference from urea in the buffer.[25] After being quantified, it was added to an aliquot of 100 µg of the extracted proteins, 100 µL of urea 8.0 mol L^{-1}. For reduction, 0.5 µL DTT 2.0 mol L^{-1} was added to the solution. Then, it was incubated for 25 min at 56 °C.

For the alkylation of the analytes, 6.1 µL of IAA 0.1 mol L^{-1} were added, and the mixture was incubated for 30 min at room temperature, protected from light. The sample was diluted until the total urea concentration was reduced to 1.6 mol L^{-1}, and 2.15 µL of 0.1 mol L^{-1} $CaCl_2$ was added.

The trypsin and endoproteinase Lys-C enzymes were added at a 1:50 (enzyme:substrate) ratio, then incubated for 18 h at 37 °C. The enzyme reaction was stopped by adding 2.0 µL of trifluoroacetic acid (TFA), resulting in a final pH below 2.0. The sample was centrifuged at 2,500 rpm for 10 min at room temperature, and the pellet was discarded.

The sample was reduced in a SpeedVac until approximately 50 µL remained. Then, 30 µL of 0.5% TFA were added. Detergents were removed from the sample using a specific column, and the sample was stored at –80 °C until analysis.

Samples from digestion in solution were diluted in TFA solution 0.5% at a concentration of 25.0 µg μL^{-1}, was aspirated by the nano high-performance liquid chromatography (nano-LC) sampler, approximately 2.0 µL of the sample, which was analyzed with a flow of 0.2 µL min^{-1}, a column (C18) of 0.1 mm, the eluents were used in the system: (A) formic acid/H_2O (1:999), (B) formic acid/ACN/H_2O (1:950:49) in an elution gradient from 2 to 50% at 165 min processing, flow rate set to 0.3 µL min^{-1} and the volume injection was 2.0 µL.

The mass spectrometer was set to MS^2 mode, positive scan, with a *m/z* range of 100-2500, a spray voltage of 3.8 kV, a capillary temperature of 250 °C, and a heater temperature of 280 °C.

Bioinformatic analysis

The data obtained from the injections in the chromatographs were imported into the Skyline software,[26] where it used the NIST mass spectral database,[27,28] and the FASTA-formatted file used for protein identification was obtained from the Uniprot library.[29,30] The following parameters were adopted: cysteine carbamidomethylation as a fixed modification, lysine acetylation, methionine oxidation as variable modifications, one missed cleavage, and automatic precursor and fragment error tolerance. The identification criteria required at least one fragment *per* peptide.

Orthologs analysis

The pathways analysis was based on the PANTHERDB classification online tools.[31] This analysis tool was used to identify the function of different proteins expressed. For the search, the Uniprot IDs with the *Rattus novergicus* genome.[28] Such a database was chosen as the reference database for the output report on biological process and molecular function information.

Statistical analysis

The statistical analysis used hypothesis testing to compare data. Analysis of variance (ANOVA) was applied, followed by Tukey's test ($p \leq 0.05$), a *post hoc* test used to determine significant differences between group means in an ANOVA setting, using Metaboanalyst 5.0.[32,33]

Additionally, principal component analysis (PCA), partial least squares-discriminant analysis (PLS-DA), and variable importance in projection (VIP-score) were applied to identify trends, similarities, and correlations among samples using the ClustVis web tool 1.0. No correction for multiples comparisons was applied; therefore, results should be interpreted as exploratory.

Results and Discussion

After analyzing all the samples in the nano-LC-MS, the chromatograms of the blanks made during the extractions were compared with the chromatograms of QCs, in order to search for possible contaminants or interferents that could generate errors in the results, and no contaminations or interferences were observed. Following this, the analysis used Skyline to obtain protein annotations.

The database contained 9296 proteins, with the most significant variation in coverage. In this work, only proteins with coverage greater than 25% were included in the statistical analyses.

Two analytical approaches were used to interpret the results. In the first, genders were not distinguished to provide an overall view of how 2,3-butanedione affects the brain. In the second, groups were separated by gender to assess how hormonal differences influence the response to exposure.

When using ANOVA ($p \leq 0.05$) without distinction of gender (Figure S1a, Supplementary Information (SI) section), it was possible to observe 55 significant proteins. The same test was then applied, separating the groups by gender. When analyzing the groups separately, the number of significant features *per* sex increased compared with when gender was not distinguished. This discrepancy can be attributed to the number of values that can cause masking or suppression during statistical calculation.

In females, a single protein showed a significant difference (Figure S1b), whereas in males, 70 proteins were differentiated. (Figure S1c). Such values suggest that the separation between the groups will occur when other chemometric tests are applied. Another important point is the need to compare only individuals of the same sex, since the ANOVA yielded values different from those observed when all samples were compared together.

To assess analytical variability and verify whether there is a separation between groups treated with 2,3-butanedione, a PCA was first performed (Figure 1).

When analyzing the graphs obtained by the comparisons, it is possible to visualize a tendency towards the grouping of the samples, but the separation between groups, emphasizing that when the analysis is performed between the sexes, the female group differs well between the control and treated groups, and despite the large dispersion of some samples from group 3 the male animals also show differentiation.

To verify whether there was a difference between the results, an additional component was used, and a 3D graph was created (Figure S2, SI section). When the three components are used to create the graph, the separation between the treated groups and the control group becomes more visible across all three statistical analyses.

The PLS-DA performance, as in the other tests, was first evaluated with all samples, without distinction by sex, and then with females and males separated (Figure 2). The result shows clustering within the groups and distance between the other groups, indicating differentiation between them and suggesting differences in protein abundance. Subsequently, a VIP score were obtained from the PLS-DA to identify which proteins have the most significant influence on group differentiation.

The cross-validation parameters were then obtained

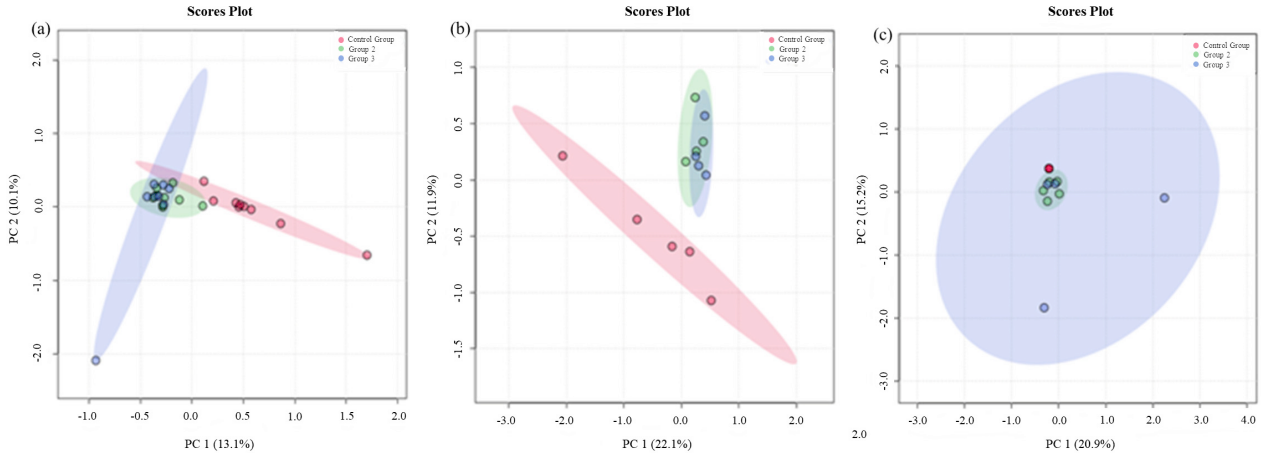

Figure 1. PCA obtained (a) without distinction of gender, (b) females, and (c) males.

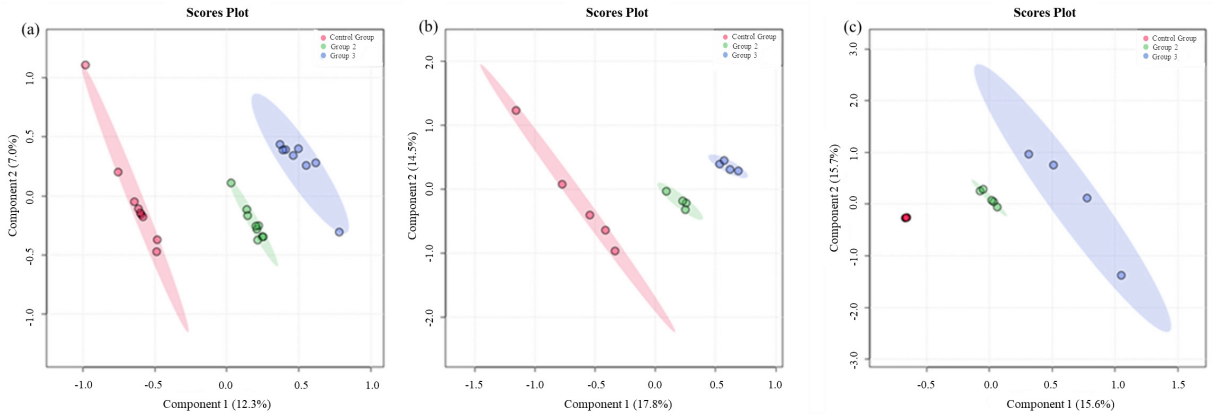

Figure 2. PLS-DA obtained (a) without gender distinction, (b) females, and (c) males.

(Figure 3). The values obtained from cross-validation for the model without distinction of gender (Figure 3a) had an excellent predictive performance (R^2), predictability (Q^2), and accuracy, exhibiting values greater than 0.8 when using more than two components in the model.[34]

When the model is observed only using the female group (Figure 3b) it is observed that the model has a good performance of R^2, showing values greater than 0.8 for any number of components used, however despite the good R^2 the model shows moderate relevance in the predictability of the model (Q^2) (greater than 0.19) according to the literature, finally this model has a moderate accuracy also regardless of the number of components used.[34]

For the male group (Figure 3c), the model shows that R^2 values are greater than 0.69 for any number of components, moderate positive Q^2 values of 0.3 or greater with two or more components, and accuracy greater than 0.4 for any number of components. Demonstrating that the model had good accuracy and prediction of the data obtained.[34]

After assessing the quality of the proposed model, the VIP score (Figure S3, SI section) was used to identify which proteins had a greater influence on group separation, thereby enabling the detection of changes in protein abundance or the presence of different proteins in certain groups.

After assessing the quality of the proposed model, the VIP score was used to identify which proteins had a greater influence on group separation, thereby enabling the detection of changes in protein abundance or the presence of different proteins in certain groups.

Figure S3 shows only 15 proteins that most influenced the separation of groups in the model. However, given the high VIP score values obtained, it is evident that a greater number of proteins exerted a significant influence and were altered.

Although the multivariate models showed satisfactory R^2 and Q^2 values, the relatively limited sample size in relation to data dimensionality warrants cautious interpretation, particularly regarding potential model overfitting.

For the continuity of this work, only annotated proteins with a VIP score greater than 1.0 were used in PantherDB. When analyzed without distinction of gender, several classes of animal proteins were altered; among the 503 most different proteins, 503 were from these classes. During the ontological analysis, a total of 78 distinct protein classes were identified (Table S1, SI section).

In addition, the absence of multiple-comparison correction reinforces the exploratory and hypothesis-generating natures of the present study, and the proteomic alterations should be interpreted as pathway-level associations rather than definitive statical evidence.

Among the 503 annotated compounds, the chemometric model identified 30 proteins annotated to pathways involving β-amyloid processing, which have been previously implicated in Alzheimer's disease according to pathway databases (Table S2). Such routes can be affected due to the acetylation that occurs through post-modifications and translations that culminate in an increase in β-amyloid, which is a pathological characteristic of Alzheimer's.[35,36]

Protein acetylation caused by exposure to 2,3-butanedione has already been reported in *in vitro* studies[37] and in *in vivo* tissues such as lungs[38] and myocardial tissue.[39] Furthermore, 2,3-butanedione has been shown to accelerate β-amyloid aggregation and induce cell death.[17]

Among the compounds noted, a large number of characteristics are also observed (Table 1) that are related to cholecystokinin receptors (CCKR) signaling and previously described as biomarkers in clinical and experimental studies of Alzheimer's disease.[40]

In addition to protein annotations associated with pathways previously implicated in Alzheimer's disease, other pathways related to neurological processes were identified based on database annotations. The model identified 52 proteins annotated commonly studied in Huntington's disease and 36 for Parkinson's disease. These results indicate that chronic exposure to 2,3-butanedione is associated with changes in brain proteomic profiles, as a molecule can cross the blood-brain barrier and interact with proteins in brain tissue.[17,41,42]

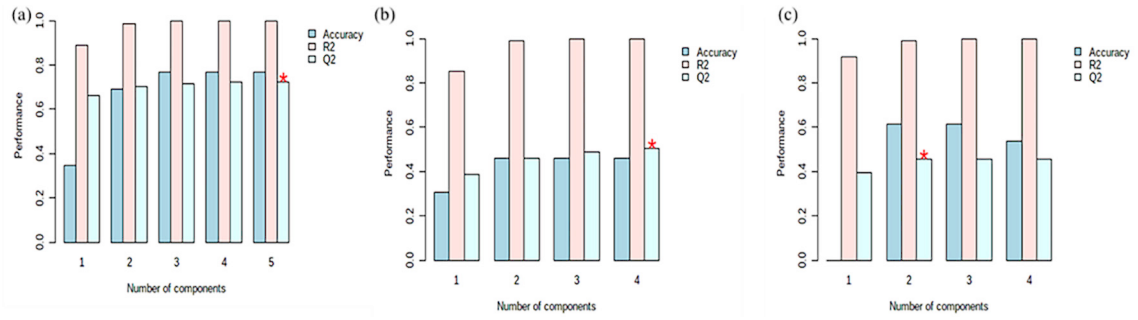

Figure 3. Cross-validation chart where (a) without gender distinction (b) females and (c) males.

Table 1. Annotated to pathways associated with neurological disorders according to PANTHERDB

Alzheimer's components found	Parkinson's components found	Huntington's components found
Alpha7 nicotinic Acetylcholine receptor	PLD2	truncated Htt
aicd	Hsp70	Hap1
pro-BACE-1	19S proteasome	Hip-12
L-Type calcium channels	UCH-L1	MLK-2
Muscarinic acetylcholine receptors	ERK	Hip-1
X11alpha	P38 MAPK	Htt
App	cyclin	pro-caspase 8
P3	Chip	Apaf-1
Fe65	Syntaxin	N-wasp
Presenilin *N*-terminal fragment	Parkin	N-cor
Pen-2	beta-synuclein	Sin3A
Mdc9	alpha-synuclein	Fip-2
Aph-1	SAPK	Duo
Tace	Ubc7	dynein complex
Tip60	Torsin A	Rac
BACE-1 pro-domain	Ubc6	C-Jun
Nicastrin	Ubch8	CBP
Abeta	Ubch7	NMDA receptor
Appalpha	Synphilin	TBP
Presenilin	Cdcrel-1	microtubule
Mapk	20s proteasome	Dynactin
C83	Dat	alpha-adaptin
BACEA-1	Pael-r	Rab8
Presenilin C-terminal fragment	Src kinase	MAPKK7
Microtubule	gamma-synuclein	cytochrome c
Appbeta	CASK	ARF
Furin	Elk-1	MAPKK4
C99	Grk	calpain
Kinesin	Fyn kinase	PSD-95
Adam10	casein kinase II	beta-tubulin
Pkc	complex i	protein fragment
–	Cul-1	SEK-1
–	Hsel10	Arfaptin-2
–	TH	Hippi
–	casein kinase I	BDNF
–	–	kainate receptor
–	–	P53
–	–	clathrin
–	–	JNK-2
–	–	polyQ Htt
–	–	Fos protein
–	–	PACSIN-1
–	–	Sp1
–	–	Synaptojanin
–	–	Akt
–	–	TAFII130
–	–	actin
–	–	caspase 8
–	–	caspase 6
–	–	GAPDH
–	–	Arp2/3 complex
–	–	caspase 3
–	–	SH3GL3

PLD2: leucine-aspartate repeat domain 2; Htt: Huntingtin protein; AICD: amyloid precursor protein intracellular domain; Hsp70: heat shock protein 70; Hap1: Huntingtin-associated protein 1; BACE-1: beta-site amyloid precursor protein cleaving enzyme 1; 19S: 19S regulatory particle of the proteasome; Hip-12: Huntingtin interacting protein 12; UCH-L1: ubiquitin C-terminal hydrolase L1; MLK-2: mixed lineage kinase 2; ERK: extracellular signal-regulated kinase; Hip-1: Huntingtin interacting protein 1; P38 MAPK: p38 mitogen-activated protein kinase; APP: Amyloid precursor protein; P3: non-amyloidogenic peptide fragment derived from APP; Chip: C-terminus of Hsc70 interacting protein; Apaf-1: apoptotic protease activating factor 1; Fe65: brain protein Fe65 (APP-binding adaptor protein); N-wasp: Neural Wiskott-Aldrich syndrome protein; N-cor: nuclear receptor corepressor; Pen-2: presenilin enhancer 2; Sin3A: SIN3 transcription regulator family member A; Mdc9: metalloproteinase-disintegrin cysteine-rich protein 9 (ADAM9); Fip-2: factor interacting with protein kinase C 2; Aph-1: anterior pharynx defective 1; SAPK: Stress-activated protein kinase; Tace: TNF-alpha converting enzyme (ADAM17); Ubc7: ubiquitin-conjugating enzyme E2 G2; Tip60: Tat-interactive protein 60 kDa (histone acetyltransferase KAT5); Rac: Ras-related C3 botulinum toxin substrate GTPase; BACE-1 (pro-domain): Pro-domain of beta-site amyloid precursor protein cleaving enzyme 1; Ubc6: Ubiquitin-conjugating enzyme E2 J1; C-Jun: Jun proto-oncogene transcription factor; UbcH8: Ubiquitin-conjugating enzyme E2 H; CBP: CREB-binding protein; Abeta: amyloid beta peptide; UbcH7: Ubiquitin-conjugating enzyme E2 L3; NMDA: *N*-methyl-*D*-aspartate receptor; TBP: TATA-binding protein; Cdcrel-1: cell division cycle related protein-like 1 (Septin family); Mapk: mitogen-activated protein kinase; C83: C-terminal fragment 83 of amyloid precursor protein; Dat: dopamine transporter; BACEA-1: Beta-site amyloid precursor protein cleaving enzyme A1; Pael-r: Parkin-associated endothelin receptor-like receptor; Rab8: Ras-related protein Rab-8; MAPKK7: Mitogen-activated protein kinase kinase 7; CASK: calcium/calmodulin-dependent serine protein kinase; ARF: ADP-ribosylation factor GTPase; Elk-1: ETS transcription factor ELK1; MAPKK4: Mitogen-activated protein kinase kinase 4; C99: C-terminal fragment 99 of amyloid precursor protein; Grk: G protein-coupled receptor kinase; PSD-95: postsynaptic density protein 95; Adam10: A disintegrin and metalloproteinase domain-containing protein 10; Pkc: protein kinase C; Cul-1: Cullin 1; SEK-1: SAPK/ERK kinase 1; Hsel10: F-box protein HSEL10; TH: tyrosine hydroxylase; Hippi: Huntingtin interacting protein interacting protein; BDNF: Brain-derived neurotrophic factor; P53: Tumor protein p53; JNK-2: c-Jun N-terminal kinase 2; polyQ: polyglutamine tract; PACSIN-1: protein kinase C and casein kinase substrate in neurons 1; Sp1: specificity protein 1 transcription factor; Akt: protein kinase B; TAFII130: TATA-box binding protein-associated factor 130; GAPDH: glyceraldehyde-3-phosphate dehydrogenase; Arp2/3: Actin-related protein 2/3 complex; SH3GL3: SH3 domain-containing GRB2-like protein 3.

When observing which proteins were noted only in females, 495 annotations were obtained, belonging to 60 different classes (Table S2). Despite the smaller number of affected routes, the Huntington's and Parkinson's disease routes have the same number of components as the model without gender distinction.

Exclusively, the female group had six pathways affected: heme biosynthesis, isoleucine biosynthesis, p53 pathway, valine biosynthesis, vitamin D metabolism, and the vitamin D pathway; these pathways are responsible for the biosynthesis of essential compounds for maintaining the life of organisms.[43-46]

Of particular note is the potential for changes in the p53 tumor suppressor pathway to alter various metabolic pathways in organisms.[47] These alterations may influence cellular regulatory and metabolic pathways involved in organismal homeostasis, highlighting the potential relevance of the observed molecular changes within an exploratory and hypothesis-generating framework.[43]

For Huntington's and Parkinson's diseases, the annotated proteins were identical across the three models (Table 1). The orthologs analysis showed that females also had a route directly linked to Alzheimer's disease. However, this differed from the analysis without sex distinction, in which the affected route corresponded to the Alzheimer's disease-presenilin pathway. This pathway is associated with molecular processes involved in amyloid-related protein processing according to database annotations, and a higher number of annotated proteins was observed compared with the previous model (Table S3, SI section).[48-52]

For males, 572 proteins belonging to 88 different pathways were identified (Table S1), and the three pathways of brain diseases were also detected (Table S4). However, despite more pathways for the diseases, they are similar to the model without gender distinction. Showing the same proteins as in Table 1.

However, the model composed only of males showed that the annotated proteins affect 13 pathways, adenine and hypoxanthine salvage pathway, anandamide degradation, axon guidance mediated by netrin, axon guidance mediated by Slit/Robo, beta2 adrenergic receptor signaling pathway, heterotrimeric G-protein signaling pathway-Gi alpha and Gs alpha mediated pathway, heterotrimeric G-protein signaling pathway-rod outer segment phototransduction, histamine H1 receptor-mediated signaling pathway, P38 Mitogen-Activated Protein (MAPK) pathway, P53 pathway feedback loops 2, PI3 kinase pathway, Proteolipid protein (PLP) biosynthesis.

It is also observed that an annotated pathway is related to p53, although its alteration can also cause the same harm already described.[43,47]

In addition to the pathways uniquely identified in each group, proteins associated with differences between groups across the proposed models were also annotated to biological processes involved in angiogenesis and vascular regulation, which are related to blood vessel maturation and maintenance according to pathway databases.[53]

Another pathway identified was the biosynthesis of adrenaline and noradrenaline, which are involved in the production of key neuromodulatory molecules important for neural signaling and brain function, according to pathway database annotations.[54]

Conclusions

The chromatographic, proteomic, and chemometric analyses performed in this study enabled the identification and differentiation of brain proteomic profiles in Wistar rats chronically exposed to 2,3-butanedione. Exposure-dependent modulation of protein expression was observed, indicating that prolonged intake of this additive influences the global molecular landscape of brain tissue. Multivariate analyses further demonstrated that sex represents an important biological variable, as male and female animals exhibited distinct proteomic response patterns across PCA, PLS-DA, cross-validation metrics, and VIP score distributions.

Among the analytical strategies evaluated, the model without sex stratification provided the most consistent overall performance for global discrimination of exposure groups, supporting its suitability for integrative assessment of brain proteomic alterations. Ontological and pathway-based analyses revealed that the dysregulated proteins were annotated to multiple biological processes involved in neuronal signaling, metabolism, cellular regulation, and stress-response mechanisms, highlighting coordinated molecular pathway modulation rather than isolated protein changes.

Importantly, the proteomic alterations identified in this work represent pathway-level associations derived from bioinformatic database annotations and should be interpreted within an exploratory, hypothesis-generating framework. No behavioral, histological, or functional neurological endpoints were assessed, and therefore the present findings do not constitute evidence of neurological disease, neurodegeneration, or pathological outcomes. Instead, this study demonstrates the applicability of proteomic profiling combined with multivariate and pathway analyses as a sensitive approach to detect molecular signatures associated with chronic exposure to 2,3-butanedione.

Collectively, these results provide a molecular foundation for future investigations integrating functional,

behavioral, and histopathological assessments, which will be necessary to further elucidate the biological significance and potential mechanisms underlying brain responses to long-term exposure to this widely used additive.

Supplementary Information

Supplementary information is available free of charge at http://jbcs.sbq.org.br as PDF file.

Data Availability Statement

All datasets are available from the authors upon request.

Acknowledgments

The authors are grateful to the Brazilian agencies: CAPES (2012/02514-9), FINEP (2013/07763-0), CNPQ (408338/2024-5, 140623/2022-1), FAPESP (2010/01404-0, 2025/26623-1, 2024/03238-2).

Author Contributions

Conceptualization, data curation and writing original draft: LXA, EC, NAA. Methodology: LXA, VGF, STBM. Formal analysis: LXA. Investigation and experimental work: LXA, NAA. Data curation, writing original draft: LXA, EC, NAA. Writing, reviewing, and editing: LG. Project supervision and administration: EC, NAA. Project funding: NAA.

References

1. Shibamoto, T.; *J. Agric. Food Chem.* **2014**, *62*, 4048. [Crossref]
2. Jedlicka, L. D. L.; Silva, J. D. C.; Balbino, A. M.; Neto, G. B.; Furtado, D. Z. S.; da Silva, H. D. T.; Cavalcanti, F. D. B. C.; van der Heijden, K. M.; Penatti, C. A. A.; Bechara, E. J. H.; Assunção, N. A.; *Biomed. Res. Int.* **2018**, *2018*, 1. [Crossref]
3. Otsuka, M.; Harada, N.; Itabashi, T.; Ohmori, S.; *Alcohol* **1999**, *17*, 119. [Crossref]
4. Taş, N. G.; Gökmen, V.; *Food Res. Int.* **2016**, *89*, 930. [Crossref]
5. Gaffney, S. H.; Abelmann, A.; Pierce, J. S.; Glynn, M. E.; Henshaw, J. L.; McCarthy, L. A.; Lotter, J. T.; Liong, M.; Finley, B. L.; *Toxicol. Rep.* **2015**, *2*, 1171. [Crossref]
6. Wang, J. Y.; Wang, X. J.; Hui, X.; Hua, S. H.; Li, H.; Gao, W. Y.; *J. Agric. Food Chem.* **2017**, *65*, 2635. [Crossref]
7. Bartowsky, E. J.; Henschke, P. A.; *Int. J. Food Microbiol.* **2004**, *96*, 235. [Crossref]
8. Cheng, H.; *Crit. Rev. Food Sci. Nutr.* **2010**, *50*, 938. [Crossref]
9. Gupta, S.; Gupta, C.; Garg, A. P.; Prakash, D.; *J. Microbiol. Exp.* **2015**, *2*, 11. [Crossref]
10. Park, Y. J.; Chae, K. H.; Rawls, H. R.; *Dent. Mater.* **1999**, *15*, 120. [Crossref]
11. Sun, G. J.; Chae, K. H.; *Polymer* **2000**, *41*, 6205. [Crossref]
12. Mishra, C.; Lambert, J.; *Asia Pac. J. Clin. Nutr.* **1996**, *5*, 20. [Crossref]
13. Jay, J. M.; *Appl. Environ. Microbiol.* **1982**, *44*, 525. [Crossref]
14. Allen, J. G.; Flanigan, S. S.; LeBlanc, M.; Vallarino, J.; MacNaughton, P.; Stewart, J. H.; Christiani, D. C.; *Environ. Health Perspect.* **2016**, *124*, 733. [Crossref]
15. Massari, J.; Fujiy, D. E.; Dutra, F.; Vaz, S. M.; Costa, A. C. O.; Micke, G. A.; Tavares, M. F. M.; Tokikawa, R.; Assunção, N. A.; Bechara, E. J. H.; *Chem. Res. Toxicol.* **2008**, *21*, 879. [Crossref]
16. Massari, J.; Tokikawa, R.; Zanolli, L.; Tavares, M. F. M.; Assunção, N. A.; Bechara, E. J. H.; *Chem. Res. Toxicol.* **2010**, *23*, 1762. [Crossref]
17. More, S. S.; Raza, A.; Vince, R.; *J. Agric. Food Chem.* **2012**, *60*, 3311. [Crossref]
18. Sadigh-Eteghad, S.; Sabermarouf, B.; Majdi, A.; Talebi, M.; Farhoudi, M.; Mahmoudi, J.; *Med. Princ. Pract.* **2015**, *24*, 1. [Crossref]
19. Park, R. M.; Gilbert, S. J.; *J. Occup. Environ. Med.* **2018**, *60*, 496. [Crossref]
20. White, A. V.; Wambui, D. W.; Pokhrel, L. R.; *Sci. Total Environ.* **2021**, *772*, 145486. [Crossref]
21. Johns, D. O.; Whittaker, C.; Cox-Ganser, J. M.; *Front. Public Health* **2022**, *10*, 1. [Crossref]
22. Mink, F. L.; *J. Geogr. Environ. Earth Sci. Int.* **2022**, *12*, 34. [Crossref]
23. Kielkopf, C. L.; Bauer, W.; Urbatsch, I. L.; *Cold Spring Harb. Protoc.* **2020**, *2020*, 136. [Crossref]
24. Sandle, T.; Satyada, R.; *Eur. J. Parenter. Pharm. Sci.* **2016**, *21*, 121. [Crossref]
25. Bradford, M. M.; *Anal. Biochem.* **1976**, *72*, 248. [Crossref]
26. Pino, L. K.; Searle, B. C.; Bollinger, J. G.; Nunn, B.; MacLean, B.; MacCoss, M. J.; *Mass Spectrom. Rev.* **2020**, *39*, 229. [Crossref]
27. Beasley-Green, A.; Bunk, D.; Rudnick, P.; Kilpatrick, L.; Phinney, K.; *Proteomics* **2012**, *12*, 923. [Crossref]
28. National Institute of Standards and Technology (NIST); *NIST Mass Spectral Library – Rat Peptide Library*; USA, 2013. [Link] accessed in February 2026.
29. Bateman, A.; Martin, M. J.; Orchard, S.; Magrane, M.; Ahmad, S.; Alpi, E.; Bowler-Barnett, E. H.; Britto, R.; Bye-A-Jee, H.; Cukura, A.; Denny, P.; Dogan, T.; Ebenezer, T. G.; Fan, J.; Garmiri, P.; da Costa Gonzales, L. J.; Hatton-Ellis, E.; Hussein, A.; Ignatchenko, A.; Insana, G.; Ishtiaq, R.; Joshi, V.; Jyothi, D.; Kandasaamy, S.; Lock, A.; Luciani, A.; Lugaric, M.; Luo, J.; Lussi, Y.; MacDougall, A.; Madeira, F.; Mahmoudy, M.; Mishra, A.; Moulang, K.; Nightingale, A.; Pundir, S.; Qi, G.; Raj, S.; Raposo, P.; Rice, D. L.; Saidi, R.; Santos, R.; Speretta, E.; Stephenson, J.; Totoo, P.; Turner, E.; Tyagi, N.; Vasudev, P.; Warner, K.; Watkins, X.; Zaru, R.; Zellner, H.; Bridge, A. J.;

Aimo, L.; Argoud-Puy, G.; Auchincloss, A. H.; Axelsen, K. B.; Bansal, P.; Baratin, D.; Batista Neto, T. M.; Blatter, M. C.; Bolleman, J. T.; Boutet, E.; Breuza, L.; Gil, B. C.; Casals-Casas, C.; Echioukh, K. C.; Coudert, E.; Cuche, B.; de Castro, E.; Estreicher, A.; Famiglietti, M. L.; Feuermann, M.; Gasteiger, E.; Gaudet, P.; Gehant, S.; Gerritsen, V.; Gos, A.; Gruaz, N.; Hulo, C.; Hyka-Nouspikel, N.; Jungo, F.; Kerhornou, A.; Le Mercier, P.; Lieberherr, D.; Masson, P.; Morgat, A.; Muthukrishnan, V.; Paesano, S.; Pedruzzi, I.; Pilbout, S.; Pourcel, L.; Poux, S.; Pozzato, M.; Pruess, M.; Redaschi, N.; Rivoire, C.; Sigrist, C. J. A.; Sonesson, K.; Sundaram, S.; Wu, C. H.; Arighi, C. N.; Arminski, L.; Chen, C.; Chen, Y.; Huang, H.; Laiho, K.; McGarvey, P.; Natale, D. A.; Ross, K.; Vinayaka, C. R.; Wang, Q.; Wang, Y.; Zhang, J.; *Nucleic Acids Res.* **2023**, *51*, D523. [Crossref]

30. UniProt Consortium (EMBL-EBI, Hinxton, United Kingdom); *UniProt Proteome UP000002494*. [Link] accessed in February 2026
31. Thomas, P. D.; Ebert, D.; Muruganujan, A.; Mushayahama, T.; Albou, L. P.; Mi, H.; *Protein Sci.* **2022**, *31*, 8. [Crossref]
32. Lu, Y.; Pang, Z.; Xia, J.; *Brief Bioinf.* **2023**, *24*, bbac553. [Crossref]
33. Pang, Z.; Chong, J.; Zhou, G.; De Lima Morais, D. A.; Chang, L.; Barrette, M.; Gauthier, C.; Jacques, P. É.; Li, S.; Xia, J.; *Nucleic Acids Res.* **2021**, *49*, W388. [Crossref]
34. Rigdon, E. E.; *Long Range Plann.* **2014**, *47*, 161. [Crossref]
35. Luo, Z.; Xu, H.; Liu, L.; Ohulchanskyy, T. Y.; Qu, J.; *Biosensors* **2021**, *11*, 1. [Crossref]
36. Seeman, P.; Seeman, N.; *Synapse* **2011**, *65*, 1289. [Crossref]
37. McGraw, M. D.; Kim, S. Y.; Reed, C.; Hernady, E.; Rahman, I.; Mariani, T. J.; Finkelstein, J. N.; *Toxicol. Lett.* **2020**, *325*, 25. [Crossref]
38. Jedlicka, L. D. L.; Guterres, S. B.; Balbino, A. M.; Neto, G. B.; Landgraf, R. G.; Fernandes, L.; Carrilho, E.; Bechara, E. J. H.; Assuncao, N. A.; *PeerJ* **2018**, *e4688*, 1. [Crossref]
39. Xiao, Y. F.; McArdle, J. J.; *Am. J. Hypertens.* **1995**, *8*, 1232. [Crossref]
40. Plagman, A.; Hoscheidt, S.; McLimans, K. E.; Klinedinst, B.; Pappas, C.; Anantharam, V.; Kanthasamy, A.; Willette, A. A.; *Neurobiol. Aging* **2019**, *76*, 201. [Crossref]
41. Haga-Yamanaka, S.; Nunez-Flores, R.; Scott, C. A.; Perry, S.; Chen, S. T.; Pontrello, C.; Nair, M. G.; Ray, A.; *eLife* **2024**, *12*, 1. [Crossref]
42. Chauhan, M. B.; Chauhan, N. B.; *J. Neurol. Neurosurg.* **2015**, *2*, 1. [Crossref]
43. Lacroix, M.; Riscal, R.; Arena, G.; Linares, L. K.; Le Cam, L.; *Mol. Metab.* **2020**, *33*, 2. [Crossref]
44. Park, J. E.; Pichiah, P. B. T.; Cha, Y. S.; *J. Obes. Metab. Syndr.* **2018**, *27*, 223. [Crossref]
45. Bayon-Vicente, G.; Marchand, E.; Ducrotois, J.; Dufrasne, F. E.; Hallez, R.; Wattiez, R.; Leroy, B.; *Front. Microbiol.* **2021**, *12*, 1. [Crossref]
46. Fujiwara, T.; Harigae, H.; *Biomed Res. Int.* **2015**, *2015*, 1. [Crossref]
47. Kruiswijk, F.; Labuschagne, C. F.; Vousden, K. H.; *Nat. Rev. Mol. Cell Biol.* **2015**, *16*, 393. [Crossref]
48. Annaert, W.; De Strooper, B.; *Annu. Rev. Cell Dev. Biol.* **2002**, *18*, 25. [Crossref]
49. Wilson, C. A.; Doms, R. W.; Lee, V. M. Y.; *J. Neurosci. Res.* **2003**, *74*, 361. [Crossref]
50. Medina, M.; Dotti, C. G.; *Cell. Signal.* **2003**, *15*, 829. [Crossref]
51. Kretschmer, M.; Rüdiger, D.; Zahler, S.; *Cancers* **2021**, *13*, 4987. [Crossref]
52. Ramesh, S.; Arachchige, A. S. P. M.; *AIMS Neurosci.* **2023**, *10*, 200. [Crossref]
53. Jiang, X.; Wang, J.; Deng, X.; Xiong, F.; Zhang, S.; Gong, Z.; Li, X.; Cao, K.; Deng, H.; He, Y.; Liao, Q.; Xiang, B.; Zhou, M.; Guo, C.; Zeng, Z.; Li, G.; Li, X.; Xiong, W.; *J. Exp. Clin. Cancer Res.* **2020**, *39*, 1. [Crossref]
54. McCutcheon, R. A.; Krystal, J. H.; Howes, O. D.; *World Psychiatry* **2020**, *19*, 15. [Crossref]

Submited: December 8, 2025
Final version online: March 10, 2026